

<https://doi.org/10.1038/s41746-025-01547-9>

Retinal fundus imaging as biomarker for ADHD using machine learning for screening and visual attention stratification



Hangnyoung Choi^{1,2,9}, JaeSeong Hong^{3,9}, Hyun Goo Kang^{4,8,9}, Min-Hyeon Park⁵, Sungji Ha², Junghan Lee^{1,2}, Sangchul Yoon⁶, Daeseong Kim⁷, Yu Rang Park³✉ & Keun-Ah Cheon^{1,2}✉

Attention-deficit/hyperactivity disorder (ADHD), characterized by diagnostic complexity and symptom heterogeneity, is a prevalent neurodevelopmental disorder. Here, we explored the machine learning (ML) analysis of retinal fundus photographs as a noninvasive biomarker for ADHD screening and stratification of executive function (EF) deficits. From April to October 2022, 323 children and adolescents with ADHD were recruited from two tertiary South Korean hospitals, and the age- and sex-matched individuals with typical development were retrospectively collected. We used the AutoMorph pipeline to extract retinal features and used four types of ML models for ADHD screening and EF subdomain prediction, and we adopted the Shapely additive explanation method. ADHD screening models achieved 95.5%–96.9% AUROC. For EF function stratification, the visual and auditory subdomains showed strong (AUROC > 85%) and poor performances, respectively. Our analysis of retinal fundus photographs demonstrated potential as a noninvasive biomarker for ADHD screening and EF deficit stratification in the visual attention domain.

Attention-deficit/hyperactivity disorder (ADHD), characterized by symptoms of inattention, impulsivity, and hyperactivity, is a prevalent neurodevelopmental disorder¹. Recent meta-analysis studies have estimated the global prevalence of ADHD to be approximately 5.41%, with rates varying across different populations and age groups². ADHD is functionally detrimental and often co-occurs with various psychiatric conditions, including substance use disorder, depression, anxiety, and an increased risk of suicide³. Early screening and timely intervention can improve social, familial, and academic functioning in individuals with ADHD⁴. Although current screening tools exhibit high diagnostic accuracy, as indicated by the area under the receiver operating characteristic (AUROC) scores, a single assessment by one informant typically lacks the necessary sensitivity and specificity (both 80%) for effective clinical application or population-level screening⁵.

ADHD diagnosis traditionally relies on a combination of clinical interviews, parent questionnaires, and neuropsychiatric testing, which are resource- and time-intensive³. Furthermore, its diagnosis at an early age presents additional challenges because of the spectrum of symptoms lacking a clear distinction between clinical diagnosis and normal behavior⁶. Moreover, several neuropsychiatric disorders, including oppositional defiant disorder, conduct disorder, autism spectrum disorder (ASD), and anxiety disorder, exhibit overlapping symptoms with ADHD⁷. This complexity and subjectivity contribute to significant variability in ADHD diagnosis and treatment decisions across different clinical settings, necessitating the development of quantifiable biomarkers for ADHD^{8,9}. In order to overcome these issues, tools such as the QbTest have been introduced, which offers a relatively quick, cost-effective, and non-invasive option for supporting ADHD diagnosis in children^{10,11}. The QbTest provides objective metrics and is more practical compared to modalities such as

¹Department of Child and Adolescent Psychiatry, Autism and Developmental Disorder Center, Severance Hospital, Yonsei University College of Medicine, Seoul, Republic of Korea. ²Department of Psychiatry and the Institute of Behavioral Science in Medicine, Yonsei University College of Medicine, Seoul, Republic of Korea. ³Department of Biomedical Systems Informatics, Yonsei University College of Medicine, Seoul, Republic of Korea. ⁴Department of Ophthalmology, Institute of Vision Research, Severance Eye Hospital, Yonsei University College of Medicine, Seoul, Republic of Korea. ⁵Department of Psychiatry, Eunpyeong St. Mary's Hospital, College of Medicine, The Catholic University of Korea, Seoul, South Korea. ⁶Department of Medical Humanities and Social Sciences, Yonsei University College of Medicine, Seoul, Republic of Korea. ⁷Yonsei University College of Medicine, Severance Hospital, Yonsei University Health System, Seoul, Republic of Korea. ⁸Present address: Bunbury and Busselton Eye Specialists, Bunbury, WA, Australia. ⁹These authors contributed equally: Hangnyoung Choi, JaeSeong Hong, Hyun Goo Kang. ✉e-mail: yurangpark@yuhs.ac; kacheon@yuhs.ac

electroencephalography (EEG) and neuroimaging. Nonetheless, it has limitations in providing comprehensive neurophysiological insights or broader biomarker applications. This emphasizes the need for novel approaches that are both efficient and capable of capturing the underlying neurobiological mechanisms of ADHD.

The pathogenesis of ADHD is complex and multifaceted and may involve neurotransmitter pathways, particularly dopamine. Additionally, considering the shared embryonic origin and similarities between the retina and brain, retinal structure and function may play a role in ADHD¹². Dopamine, which plays a crucial role in ADHD symptomatology, is involved in multiple aspects of retinal function, including visual processing and attention¹³. Abnormalities in electroretinogram (ERG) parameters have been identified in individuals with various mental disorders^{14,15}, potentially related to cerebral dopaminergic pathways¹⁶. Functionally, individuals with ADHD show increased retinal noise, as measured by pattern ERG¹⁷, decreased a-wave amplitude in females¹⁸, and increased b-wave amplitude¹⁹.

Dopamine receptors are present in diverse retinal neuronal types, including horizontal, amacrine, and ganglion cells, where they play crucial roles in synaptic formation, retinal development, and adaptive processes^{20,21}. Pieces of evidence suggest that dopamine enhances retinal blood flow and regulates vascular endothelial cells, possibly affecting vascular permeability and structural remodeling^{22,23}. These observations indicate the dual role of dopaminergic signaling in regulating both retinal function and structural attributes, such as vessel density and optical structure, which are associated with ADHD pathophysiology. Promising association links between retinal characteristics and ADHD could offer advanced understanding for biomarker research and diagnostic approaches.

Previous studies on retinal structure in ADHD have reported reduced thickness of the retinal nerve fiber layer (RNFL) compared with typical development. However, these studies involved limited sample sizes, and the results remain controversial^{13,24}. Nonetheless, significant differences observed in specific areas of the retinal layers, including inferior ganglion cells and nasal macular thickness, indicate an association between altered retinal structure and ADHD²⁵. Changes in retinal structure reflect abnormalities in the brain in various psychiatric disorders¹². Retinal fundus photography is a widely used tool to investigate structural change. As a screening tool, it has several advantages: rapidity, non-invasiveness, well-tolerability, reproducibility, and cost-effectiveness.

Machine learning (ML) techniques have demonstrated great potential for analyzing retinal photographs owing to their ability to automatically extract detailed features from complex images and efficiently handle high-dimensional data, thus enhancing the accuracy, speed, and scalability of medical diagnostics. ML techniques are invaluable for identifying subtle biomarkers in conditions such as ADHD. Previous studies using ML models to distinguish ADHD from normal controls based on various modalities such as eye tracking data, EEG, and neuroimaging have shown promising outcomes²⁴. However, their use in real-world clinical practice is limited, as they are time-consuming and need expensive tests requiring considerable cooperation from individuals with ADHD. Recently, we demonstrated that a deep ensemble ML model using only retinal fundus photographs could be a potential objective screening tool that robustly discriminates between children with ASD and typical development²⁶.

Considering the role of dopamine in both retinal function and ADHD symptomatology, we hypothesized that retinal structure could serve as a potential biomarker for ADHD diagnosis and stratification. This study aimed to develop ML models using features extracted from retinal fundus photographs as a reliable screening tool for ADHD. We also assessed the ability of these ML models to stratify individuals with ADHD according to executive function (EF) deficits using the comprehensive attention test (CAT)²⁷.

Results

Study population

This study analyzed 1108 fundus photographs from 646 participants (<19 years). For children with ADHD, 334 images out of 888 images from 445

ADHD participants and 32 images out of 586 images from 345 participants were excluded. This exclusion was followed by the result of the “Image Quality Assessment” process in the AutoMorph pipeline. The mean age of the participants was 9.5 years ([SD] 3.2 years; 498 boys [77.1%]). The ADHD group included 323 participants (554 eyes)—153 from the Eunpyeong St. Mary’s Hospital (221 images) and 170 from Severance Hospital (333 images). The TD group included 323 age- and sex-matched participants (554 images). Among the participants with ADHD, 168 completed the Korean ADHD Rating Scale (K-ARS), with median scores of 13.0 (inattentive), 12.5 (hyperactive), and 25.0 (total). A subset of 118 participants with ADHD underwent the CAT (detailed results are shown in Table 1). Supplementary Fig. 1 and Supplementary Fig. 2 illustrate the study design and participant flow. For the age- and sex-distribution matched ADHD and ASD, we used 314 photographs and 308 photographs from 160 participants with ADHD and 160 participants with ASD.

ADHD screening model performance

All ML models demonstrated excellent performance in distinguishing children with ADHD from TD. Random Forest (RF), extreme gradient boosting (XGBoost), extra trees classifier (EXT), and logistic regression (LR) models achieved AUROC values of 95.5% (95% CI 94.6–96.5%), 96.9% (95% CI 96.2–97.7%), 96.4% (95% CI 95.6–97.2%), and 96.5% (95% CI 95.7–97.4%), respectively (Fig. 1). The best-performing model, XGBoost, showed high sensitivity of 91.6% (95% CI 89.7–93.7%) and specificity of 92.0% (95% CI 90.1–93.9%), with balanced positive predictive value of 91.8% (95% CI 90.5–93.2%), negative predictive value of 91.9% (95% CI 90.1–93.9%), and F1-score of 91.7% (95% CI 89.8–93.6%). The model demonstrated good calibration with the negative log-likelihood (NLL) of 0.24 (95% CI 0.2–0.27) and the Brier score of 0.07 (95% CI 0.06–0.07). The detailed performance metrics and their thresholds achieved with Youden Index for all models are presented in Supplementary Table 1, and the performances for each fold dataset are provided in Supplementary Table 2. The results for discriminating ADHD and ASD are provided in Supplementary Note 1.

Feature importance in ADHD screening

We analyzed the Shapley additive explanations (SHAP) feature importance of XGBoost, which demonstrated the highest performance for ADHD screening, to elucidate the key distinguishing features between ADHD and TD. Figure 2a presents a beeswarm plot of the SHAP values, illustrating the directional impact of each feature on the output of the model. A positive SHAP value indicates the contribution of the feature to the ADHD classification, whereas the color gradient represents the magnitude of the feature. Notably, higher values of vessel density, average vessel width, and arterial vessel density in Zone B were strongly associated with ADHD classification. Conversely, lower values of the arterial fractal dimension, average vein width, overall fractal dimension, and cup-disc ratio were indicative of ADHD. Figure 2b presents a bar plot displaying the average magnitude of the absolute SHAP values, quantifying the overall impact of each feature on the predictions, regardless of the direction. With an average SHAP value of 1.6, vessel density had the greatest impact among the features. Following this, the second, third, and fourth most significant features were arterial fractal dimension, average width, and vein average width, all of which had average SHAP values of more than 1.0.

EF subdomain prediction

Models predicting EF subdomains in ADHD exhibited varying performances across different attention measures (Fig. 3). The visual selective attention (VSA)-omission errors (OE) domain, with a cutoff point of attention quotients (AQ) of 80, demonstrated the highest median performance (median 87%, IQR 85.2–88.5%). The VSA domain consistently outperformed other domains, with five out of 15 models achieving AUROC values of $\geq 80\%$ and 14 models achieving $\geq 70\%$. The sustained attention response task (SART) domain also demonstrated good performance, with all 15 models achieving AUROC values of $> 70\%$ and four models achieving $> 80\%$. In contrast, the auditory selective attention (ASA) domain

Table 1 | Baseline characteristics of participants

	Participants with ADHD (<i>n</i> = 323)	Participants with TD (<i>n</i> = 323)
Age, mean (SD)	9.5 (3.2)	9.5 (3.2)
Sex (male), <i>n</i> (%)	249 (77.1%)	249 (77.1%)
Korean ADHD Rating Scale, <i>n</i> (%)	168 (48.9%)	
Inattention score	13 (9–17)	
Hyperactivity and Impulsivity score	12.5 (8–17)	
Total score	25 (18–33)	
Comprehensive attention test, <i>n</i> (%)	118 (36.5%)	
Visual attention test - omission errors	102 (98–107)	
Visual attention test - commission errors	103 (94.3–115)	
Visual attention test - response time	86 (71–99)	
Visual attention test - response time standard deviation	87.5 (70–100)	
Auditory attention test - omission errors	107 (100–110.8)	
Auditory attention test - commission errors	102 (100–111)	
Auditory attention test - response time	87 (71–100)	
Auditory attention test - response time standard deviation	91 (74.3–105)	
Sustained attention to response task - omission errors	88 (70–100)	
Sustained attention to response task - commission errors	91 (70–100)	
Sustained attention to response task - response time	75 (70–89.8)	
Sustained attention to response task - response time standard deviation	70 (70–89)	
Flanker task - omission errors	100 (85–104)	
Flanker task - commission errors	97 (74–100)	
Flanker task - response time	90 (73.3–99.8)	
Flanker task - response time standard deviation	95 (79–100)	

Data are presented as the mean (SD), *n* (%), or median (IQR). *ADHD* attention-deficit/hyperactivity disorder, *TD* typical development, *SD* standard deviation, *IQR* interquartile range

performed poorly, with only one and eight models achieving AUROC values of > 80% and > 80%, respectively. Notably, only two subdomains were available in the flanker task (FT) domain, with both exhibiting AUROC values of > 80%. However, models predicting severity based on the K-ARS scores were less successful, with AUROC values of < 60% (Supplementary Fig. 3), and the predicting ASD and ADHD show low performance, with the highest AUROC of 63.0% (95% CI 60.2–66.0%) (Supplementary Note 1).

Discussion

This study used ML models to classify the retinal features extracted from color fundus photographs of children with ADHD and TD. All models, including RT, XGBoost, EXT, and LR, demonstrated excellent performance with average AUROC values of 95.5–96.9% for distinguishing the two groups. Compared to other ML approaches for ADHD classification, such as those based on continuous performance test (CPT), event-related potential (ERP), EEG, eye movement, and imaging modalities, our model offers a unique combination of non-invasiveness, accessibility, and scalability. For instance, CPT-based models, which assess attention and impulsivity through task performance, typically achieve an accuracy value of 87% but do not capture structural biomarkers²⁸. While effective (AUROC 82–99%), ERP and EEG-based models require specialized equipment and participants' cooperation, limiting their scalability^{29–32}. Eye movement models are task-specific and show moderate classification success (AUC: 86–92%; accuracy: 76.3%)^{33,34}, while imaging-based models (AUROC 82%), such as magnetic resonance imaging (MRI) (i.e. structured MRI, resting-state fMRI, task-based fMRI), provide detailed neurodevelopmental insights but are resource-intensive²⁴.

Notably, earlier high-accuracy models typically relied on a diverse set of variables, each contributing incrementally to differentiating subjects^{35–37}. However, our approach simplifies the analysis by focusing exclusively on retinal photographs. This single-source data strategy enhances the clarity and utility of our models. Moreover, robust performance was observed in

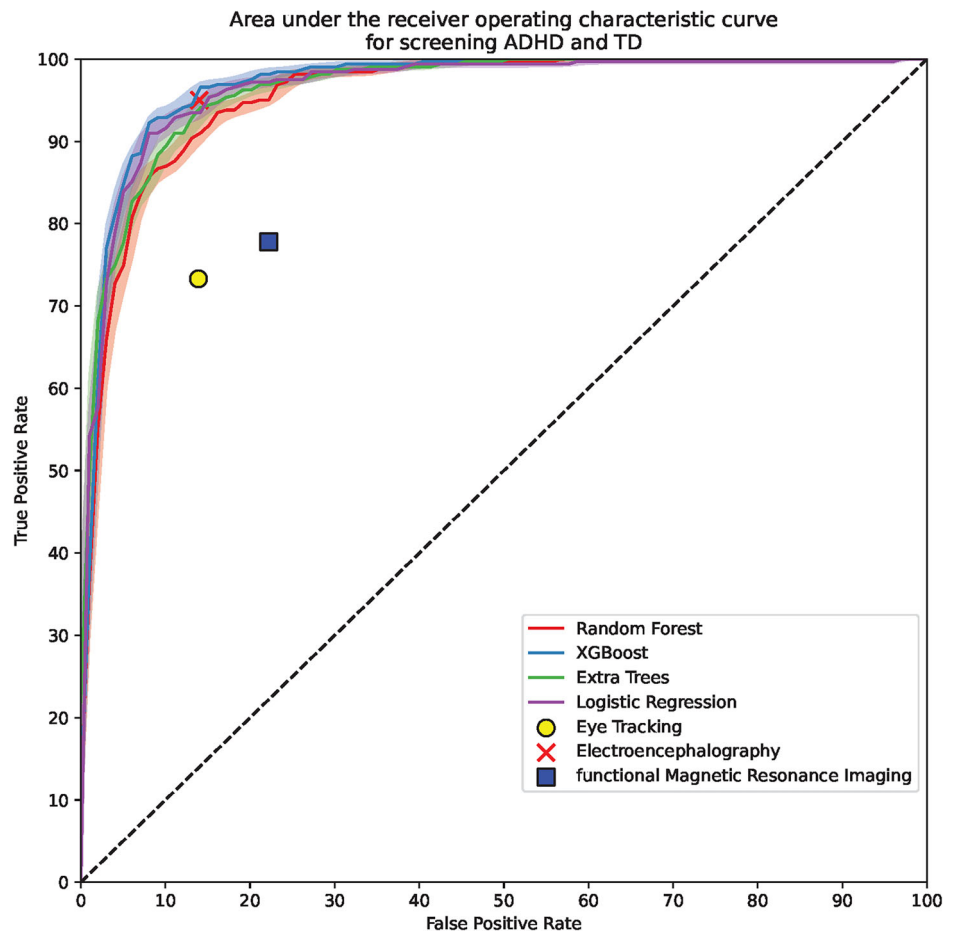
stratifying the visual attention domains (the VSA and SART domains), with the highest AUROC values of 87.3% and 85.8% for each task, respectively. These findings underscore the promising utility of retinal images for ADHD screening and demonstrate the interpretability and practicality of the methodology.

Our study identified key features, primarily encompassing vessel density, average vessel width, and optic disc characteristics, for distinguishing children with ADHD from those with TD. Children with ADHD exhibited denser and thicker overall retinal vasculature than children with TD, with a notable exception in the peripapillary area (Zone B), where the arterial vessels were dense but thinner. Furthermore, both cup and disc sizes tended to be smaller in children with ADHD. These findings are consistent and expand upon previous research, reporting higher choroidal thickness in individuals with ADHD³⁸, as well as smaller optic discs, reduced neuroretinal rim area, and decreased tortuosity of the retinal artery³⁹.

Detectable microstructural alterations in cortical regions and diffuse white matter of ADHD brains may be reflected in the retinal structure, considering that the retina is an extension of the central nervous system (CNS)^{40–42}. However, unlike most CNS neurons with typical myelination, RNFL primarily consists of unmyelinated axons originating from retinal ganglion cells. These axons undergo myelination within the optic nerve, forming a white matter tract that transmits visual information to the lateral geniculate nucleus⁴³. Consequently, relying solely on anatomical connectivity may be insufficient to explain the observed structural alterations in the retina.

Alterations in the retinal structure of ADHD may be associated with dysregulated dopaminergic signaling. Dopamine is hypothesized to play a significant role in retinal development, synapse formation and signaling, adaptive processes^{44–49}, and vascular remodeling through its actions on retinal dopamine receptors^{22,23,50}. Dysfunctional dopamine signaling, a well-established contributor to ADHD pathophysiology, affects attention, impulsivity, and EF⁵¹. Our findings correspond to this hypothesis, revealing

Fig. 1 | AUROC plot of ADHD screening based on retinal features. AUROC curves of the four machine learning models for distinguishing between ADHD and TD. ADHD, attention-deficit/hyperactivity disorder; TD, typical development; Random Forest, random forest classifier; XGBoost, extreme gradient boosting classifier; Extra Trees, extra tree classifiers. Circle, “X”, and square indicate the AUROC values of eye tracking, electroencephalography, and functional magnetic resonance imaging.



significant neurovascular abnormalities in the retina in children with ADHD. Inflammatory markers beyond the CNS may also contribute to ADHD-related vascular change. A recent meta-analysis reported elevated interleukin-6 (IL-6) levels and reduced tumor necrosis factor- α (TNF- α) levels in individuals with ADHD, suggesting a role of inflammation in ADHD pathophysiology⁵². Such inflammatory states, including altered IL-6 and TNF- α levels, may play a role in systemic vascular remodeling, which could potentially influence retinal vascular structure in individuals with ADHD^{53,54}. There is further evidence to suggest that retinal ganglion cells are particularly susceptible to these cytotoxic effects⁵⁵.

Functionally, electrophysiological measures such as the b-wave and oscillatory potentials in ERG have revealed increased background retinal noise in individuals with ADHD¹⁷. This elevated noise in the retina corresponds with disruptions in the brain, where reduced noise facilitates focused neuronal activation across networks that govern cognitive tasks⁵⁶. Studies by Dubois et al., and Lee et al., have also demonstrated specific alterations in ERG measures, including decreased a-wave amplitude in females with ADHD, increased b-wave amplitude, and abnormal oscillatory potentials^{18,19}. These findings suggest that ADHD-related neural disruptions are not limited to the CNS but extend to the retina, a neurodevelopmentally and functionally connected structure^{17–19}.

Notably, reduced cortical dopamine levels are associated with diverted attention and resources, whereas excessively high dopamine levels can compromise neural network functionality⁵⁷. For instance, dysfunction of the visual cortex striatum default mode network pathway may be associated with potential inattentiveness symptoms in ADHD, likely resulting from prolonged abnormal input from the retina⁵⁸. These findings emphasize the relevance of balanced dopamine levels for optimal brain network function, indicating that both

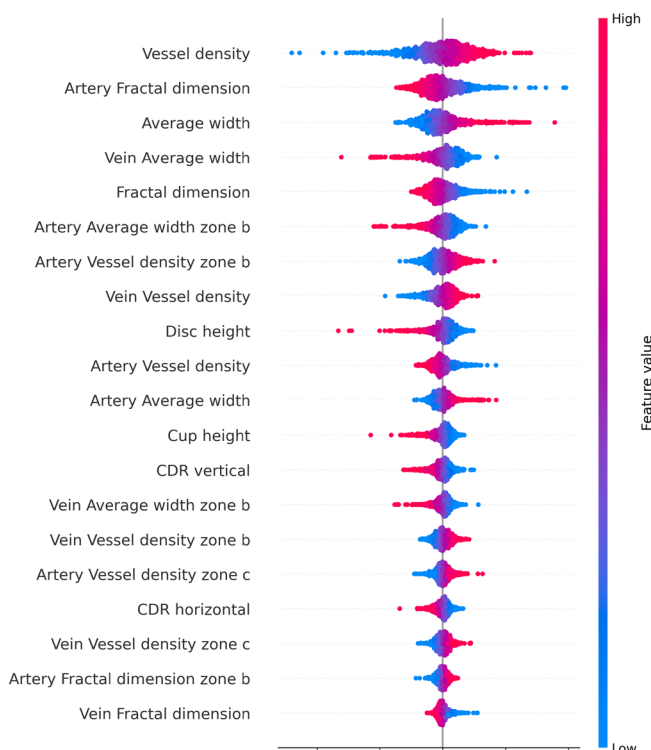
brain and retinal structures are involved in a shared neurodevelopmental process.

In this study, the prediction of severity was considerably more feasible based on the visual tasks (VSA and SART) than on the auditory tasks, as demonstrated by the significantly higher performance of the subgroups. In particular, 14 out of 15 subgroups exhibited AUROC values of >0.7 in the VSA domain, with all 15 subgroups exhibiting AUROC values of >0.7 in the SART domain. Conversely, only eight subgroups achieved AUROC values of >0.7 in the ASA domain. This finding aligns with previous research that highlights more pronounced executive deficits in tasks requiring visual attention, emphasizing the moderate effectiveness of the ML model using retinal photographs for EF deficit prediction in ADHD^{59,60}.

In ADHD, stimulus encoding and processing (perceptual functions) are closely intertwined with response selection (EF), suggesting that deficits in perceptual functions are associated with impairments in EF⁶¹. The intricate pathway of visual processing, from retinal stimulation to saccadic target formation in the posterior parietal cortex, involves the complex integration of sensory input and motor output necessary for precise control of eye movements⁶². Interestingly, abnormal saccadic movements commonly observed in individuals with ADHD are related to deficits in response inhibition and inattention⁶³. Interventions such as eye-tracking exercises and quiet eye training have shown potential in improving inhibitory control in individuals with ADHD, stressing the critical association between visual processing and EF^{64,65}.

Few studies have directly examined the relationship between retinal structure and cognitive function in children. Provost et al. reported an inverse correlation of the dense retinal microvascular network with behavioral outcomes and sustained attention ability, which is consistent with our results⁶⁶. However, no significant correlation between RNFL thickness and symptom severity of ADHD or EF performance has been reported. This

a) Beeswarm plot of the SHAP values



b) Average magnitude of the absolute SHAP values

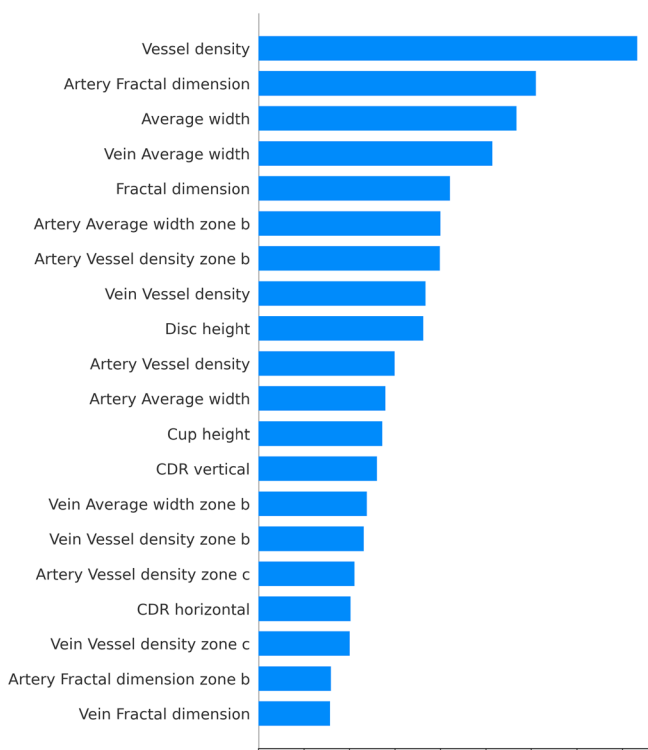


Fig. 2 | Feature importance analysis for ADHD classification using SHAP values of XGBoost classifier. a Beeswarm plot illustrating the directional impact of each feature on model predictions. Positive SHAP values indicate contributions toward ADHD classification, while negative SHAP values indicate contributions toward TD classification. The x-axis represents SHAP value magnitudes, and the color gradient

(red to blue) represents the feature values, with red indicating higher values and blue indicating lower values. **b** Bar plot showing the average magnitude of absolute SHAP values for the top 20 features. Longer bars indicate features with greater overall influence on the model's predictions. ADHD attention-deficit/hyperactivity disorder, TD typical development, SHAP Shapley additive explanations.

indicates that although RNFL measurements may reflect certain neural characteristics of ADHD, they do not directly correlate with functional impairments⁶⁷. Our ML model successfully stratified EF severity using retinal photograph analysis but did not achieve stratification of symptom severity as measured using the K-ARS. This corroborates the complexity of ADHD diagnosis and suggests that retinal biomarkers, although potentially valuable, should be considered complementary to conventional diagnostic tools, such as the DSM-5.

Nevertheless, the correlation between the retinal structure and EF deficits in ADHD supports its potential as a therapeutic biomarker. Notably, methylphenidate (MPH), a dopamine reuptake inhibitor, enhances various aspects related to attention in individuals with ADHD⁶⁸, and significant differences in terms of parafoveal thickness were observed between the ADHD and TD groups, indicating a possible influence of MPH on retinal circulation⁶⁹. Additionally, retinal thickness was positively correlated with the duration of MPH use, with greater retinal thickness in children undergoing treatment with MPH for 24 months⁷⁰. Complementing these clinical findings, the animal study has shown that MPH exerts beneficial effects on the retina by reducing microgliosis, mitigating blood-retinal barrier dysfunction, and attenuating inflammatory responses⁷¹.

This study has some limitations. First, the dataset was derived from two hospitals in South Korea, potentially limiting the generalizability of our findings to broader populations. Future validation with external datasets encompassing diverse geographical and demographic settings is essential to confirm the global applicability of retinal biomarkers in ADHD screening and visual attention stratification. Nevertheless, our study provides robust preliminary evidence for the potential utility of retinal photographs in this context. Second, while retinal photographs were effective in identifying structural differences associated with ADHD, the two-dimensional nature

of these images provides limited information. Although optical coherence tomography (OCT), incorporating three-dimensional imaging techniques, has been explored in ADHD and ASD populations, its results have been inconsistent^{25,72}. Retinal photography, due to its rapidity and accessibility, may serve as a practical screening tool. On the one hand, advanced imaging modalities such as optical coherence tomography angiography (OCT-A) could complement retinal photography by capturing microvascular changes, presenting an alternative for further biomarker investigation. Third, our study focused on participants within a narrow age range (mean: approximately 9 years), which limits the generalizability of the findings to other developmental stages. Future research should investigate whether retinal biomarkers vary across age groups, considering the developmental trajectories of ADHD.

Fourth, we excluded participants with comorbid neuropsychiatric conditions to minimize confounding effects. While this approach was necessary to isolate ADHD-related retinal features, it limits the relevance of our findings to clinical populations, where comorbidities such as ASD, anxiety disorders, and intellectual disabilities are prevalent. Investigating how retinal biomarkers differ in individuals with ADHD and co-occurring conditions remains an important area for future research. Lastly, we conducted an exploratory analysis to examine the specificity of retinal biomarkers in distinguishing ADHD from ASD (Supplemental note 1). The analysis revealed limited classification performance, suggesting that retinal biomarkers alone may lack sufficient specificity for differentiating between neurodevelopmental disorders. The results reflect the overlapping morphological and functional features commonly observed in ADHD and ASD, which share genetic and neurodevelopmental pathways^{73,74}. Further studies should consider multimodal approaches that integrate retinal imaging with neuroimaging, electrophysiological measures, or other biomarkers to enhance specificity.

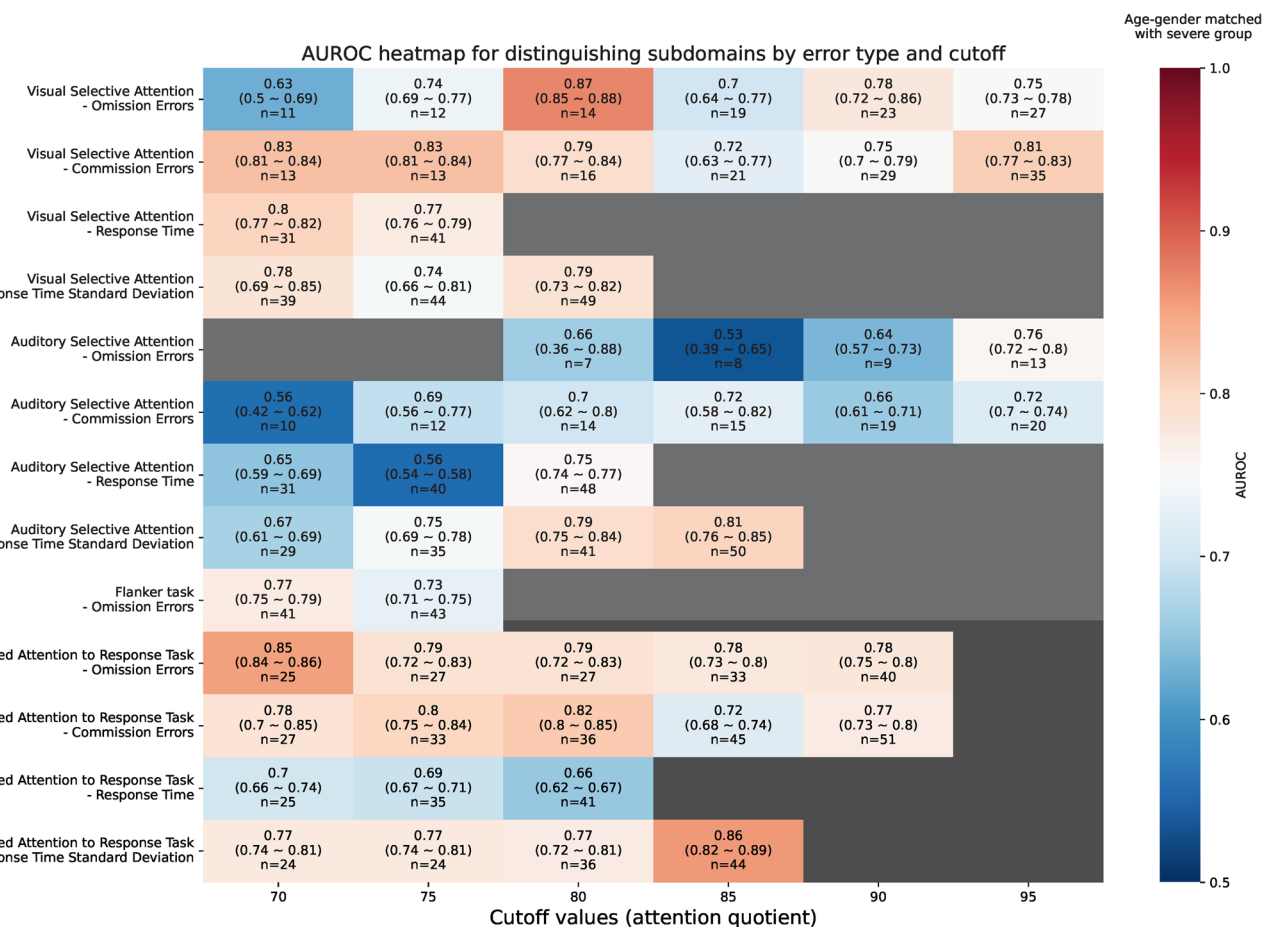


Fig. 3 | Performances of distinguishing subdomains of executive function deficits using comprehensive attention tests in ADHD based on retinal features. Complete results for distinguishing subdomains of executive function deficits using comprehensive attention tests in ADHD based on retinal features. The heatmap depicts the performance based on AUROC values, with red indicating higher performance and blue indicating lower performance. The gray background color indicates no age- and sex-matched undersampling because of the large data size for VSA-RT, ASA-RT, and others or insufficient data for ASA-OE and ASA-CE. AQ values represent the normalized scores for each executive function, with a mean of

100 and a standard deviation of 15. Cutoff values were set in 5-point increments between 70 and 100 for the analysis. These cutoffs were used to divide the ADHD group into two subgroups for executive function stratification. We developed multiple models to distinguish 96 subdomains with 16 AQ values and six incremental cutoff values ranging from 70 to 95 with five points. ADHD attention-deficit/hyperactivity disorder, AUROC area under the receiver operating characteristic curve, AQ attention quotient, VSA visual selective attention, ASA auditory selective attention, OE omission errors, CE commission errors (CE), RT mean reaction time.

This is the first ML study to use retinal photographs to distinguish ADHD from TD and stratify ADHD subgroups. Our ML model demonstrated high diagnostic accuracy, sensitivity, and specificity, suggesting that retinal structure could be a promising biomarker of ADHD, reflecting the severity of EF impairment.

Methods

Study design and participants

Children and adolescents with ADHD were recruited from two South Korean hospitals—Severance Hospital and Eunpyeong St. Mary's Hospital—between April and October 2022. ADHD was diagnosed based on the DSM-5 criteria¹. Retinal photographs of age- and sex-matched typically developing children were retrospectively collected from the Department of Ophthalmology, Severance Hospital, between December 2007 and July 2024. Retinal photographs were taken from both eyes in all participants, except for those children with lower compliance who were unable to complete photos for both eyes, and as such only the single photo from one eye was used. The fundus photo field size was 50 degrees and was captured in undilated eyes. The individuals with major psychiatric disorders (e.g., bipolar disorder, autism spectrum disorder, or conditions within the schizophrenia spectrum and other psychotic disorders), neurological disorders (e.g., epilepsy, encephalitis, demyelinating disease, or traumatic brain

injury), and eye diseases that may affect the retinal fundus (e.g., glaucoma, retinopathy of prematurity, or ophthalmic surgical history) were excluded. All ADHD participants were drug-naïve at the time of the study, with no history or current use of stimulant medications (e.g., methylphenidate), non-stimulant ADHD medications, or any other psychotropic drugs. This study was approved by the Institutional Review Board of Severance Hospital, Yonsei University, Republic of Korea (IRB number: 4-2022-0297). Written informed consent was obtained from all participants with ADHD, whereas the requirement for consent from participants with typical development (TD) was waived owing to the use of retrospective and de-identified data. The study complied with the STARD guidelines (Supplementary Note 3)⁷⁵.

Data pre-processing and feature extraction

Features from single retinal photographs were analyzed using AutoMorph, an automated retinal neurovascular morphology quantification pipeline⁷⁶. This deep learning-based approach extracted features from anatomical segmentations of the optic disc/cup, vessels, and artery/vein structures considering the images' resolution with their devices. We resized the original retinal photographs into the size of 600 × 600 with the linear interpolation method⁷⁷. Additional information extracted from AutoMorph package is provided in Supplementary Table 3. The

extracted feature values were standardized before inputting them into the machine learning models.

Model development

We developed four ML models—random forest classifier (RF), extreme gradient boosting classifier (XGBoost), extra trees classifier (EXT), and logistic regression (LR)⁷⁸—for screening ADHD from TD and predicting EF subdomains in ADHD using CAT scores. The CAT, a computer-based continuous performance test, assessed four subsets of attention: visual selective attention (VSA), auditory selective attention (ASA), sustained attention response task (SART), and flanker task (FT). Each subset provides four indicators: omission errors, commission errors, mean reaction time, and standard deviation of reaction time²⁷, which were normalized to attention quotients (AQs) adjusted for age and sex. More detailed information on CAT is provided in Supplementary Note 4. We stratified individuals with ADHD into subgroups based on their AQ scores and developed multiple models to distinguish the 96 subdomains. Additionally, we developed models to stratify ADHD severity using the Korean ADHD Rating Scale (K-ARS), including three subsets of inattention, hyperactivity, and total scores, with cutoff values of median and numbers at the 75% quantile⁷⁹. We also conducted age- and sex-distribution matched ADHD and ASD dataset, and developed models to distinguish them. Detailed information on hyperparameter settings is provided in the Supplementary Table 4.

Statistical analysis and model performance

We implemented a five-fold stratified cross-validation, allocating 60%, 20%, and 20% data for training, validation, and testing in each fold, respectively. We trained the models using default settings while systematically varying the number of estimators from 100 to 1000 to enhance generalizability. Considering that ADHD and its subdomains are participant-level constructs, we aggregated the probabilities at the participant level. In cases when image acquisition failed or an image was excluded because of poor quality, we used the available single image for prediction, ensuring a comprehensive analysis of all participants. We evaluated model performance using comprehensive metrics, including area under the receiver operating characteristic curve (AUROC), sensitivity, specificity, positive and negative predictive values, and F1-score at the Youden index. Model calibration was assessed using the negative log-likelihood (NLL) and the Brier score²⁷. To ensure robust estimates, we calculated 95% confidence intervals for all metrics using bootstrapping with 1000 resamples. Differences in clinical variables between the two groups were assessed using independent *t*-tests or χ^2 tests. Age- and sex-matched undersampling methods were used if the final subset of the groups exhibited $p < 0.05$. Detailed information on performance evaluation metrics is provided in the Supplementary Note 2.

Model interpretation and technical details

To elucidate the relative importance of different retinal features in our models, we employed the Shapley additive explanations (SHAP) method⁸⁰. This approach facilitated a quantitative evaluation of feature importance for the best-performing model, offering insights into the specific retinal characteristics most predictive of ADHD. All analyses were conducted using Python (version 3.9.15), leveraging the Scikit-Learn (version 1.4.1) and XGBoost (version 2.0.3) libraries for ML implementations. Data analysis was performed between July and August 2024. External model validation using an independent dataset was not performed.

Data availability

We used data from participants with attention-deficit/hyperactivity disorder (ADHD) from the Open AI Dataset Project (AI-Hub, South Korea). All retinal image data with ADHD is publicly accessible on “AI-Hub (www.aihub.or.kr).” The study data can be obtained from either of the corresponding authors (YRP: yurangpark@yuhs.ac or K-AC: kacheon@yuhs.ac) upon reasonable request.

Code availability

The code that supports the findings of this study is openly available at: <https://github.com/DigitalHealthcareLab/24ADHDBRetina>.

Received: 29 October 2024; Accepted: 2 March 2025;

Published online: 17 March 2025

References

1. American Psychiatric Association. *Diagnostic and Statistical Manual of Mental Disorders: DSM-5*. (American Psychiatric Association, Arlington, VA, 2013).
2. Cortese, S. et al. Incidence, prevalence, and global burden of ADHD from 1990 to 2019 across 204 countries: data, with critical re-analysis, from the Global Burden of Disease study. *Mol. Psychiatry* **28**, 4823–4830 (2023).
3. Faraone, S. V. et al. The World Federation of ADHD International Consensus Statement: 208 Evidence-based conclusions about the disorder. *Neurosci. Biobehav. Rev.* **128**, 789–818 (2021).
4. Sonuga-Barke, E. J., Koerting, J., Smith, E., McCann, D. C. & Thompson, M. Early detection and intervention for attention-deficit/hyperactivity disorder. *Expert Rev. Neurother.* **11**, 557–563 (2011).
5. Mulraney, M. et al. Systematic review and meta-analysis: screening tools for attention-deficit/hyperactivity disorder in children and adolescents. *J. Am. Acad. Child Adolesc. Psychiatry* **61**, 982–996 (2022).
6. Hinshaw, S. P. Attention Deficit Hyperactivity Disorder (ADHD): Controversy, Developmental Mechanisms, and Multiple Levels of Analysis. *Annu. Rev. Clin. Psychol.* **14**, 291–316 (2018).
7. Egger, H. L. & Angold, A. Common emotional and behavioral disorders in preschool children: presentation, nosology, and epidemiology. *J. Child Psychol. Psychiatry* **47**, 313–337 (2006).
8. Visser, S. N. et al. Trends in the Parent-Report of Health Care Provider-Diagnosed and Medicated Attention-Deficit/Hyperactivity Disorder: United States, 2003–2011. *J. Am. Acad. Child Adolesc. Psychiatry* **53**, 34–46.e2 (2014).
9. Lyhmann, I. et al. Variation in attitudes toward diagnosis and medication of ADHD: a survey among clinicians in the Norwegian child and adolescent mental health services. *Eur. Child Adolesc. Psychiatry* **32**, 2557–2567 (2023).
10. Hollis, C. et al. The impact of a computerised test of attention and activity (QbTest) on diagnostic decision-making in children and young people with suspected attention deficit hyperactivity disorder: single-blind randomised controlled trial. *J. Child Psychol. Psychiatry* **59**, 1298–1308 (2018).
11. Gustafsson, U. & Hansen, M. QbTest in the clinical assessment of attention deficit hyperactivity disorder: A review of the evidence. *Ment. Health Sci.* **1**, 270–281 (2023).
12. Silverstein, S. M., Demmin, D. L., Schallek, J. B. & Fradkin, S. I. Measures of retinal structure and function as biomarkers in neurology and psychiatry. *Biomark. Neuropsychiatry* **2**, 100018 (2020).
13. Bellato, A. et al. Association between ADHD and vision problems. A systematic review and meta-analysis. *Mol. Psychiatry* **28**, 410–422 (2023).
14. Youssef, P., Nath, S., Chaimowitz, G. A. & Prat, S. S. Electroretinography in psychiatry: A systematic literature review. *Eur. Psychiatry* **62**, 97–106 (2019).
15. Almonte, M. T., Capellán, P., Yap, T. E. & Cordeiro, M. F. Retinal correlates of psychiatric disorders. *Ther. Adv. Chronic Dis.* **11**, 2040622320905215 (2020).
16. Lavoie, J. et al. The Electroretinogram as a Biomarker of Central Dopamine and Serotonin: Potential Relevance to Psychiatric Disorders. *Biol. Psychiatry* **75**, 479–486 (2014).
17. Bubl, E. et al. Elevated Background Noise in Adult Attention Deficit Hyperactivity Disorder Is Associated with Inattention. *PLOS ONE* **10**, e0118271 (2015).

18. Dubois, M.-A. et al. Evaluation of electroretinography (ERG) parameters as a biomarker for ADHD. *Prog. Neuropsychopharmacol. Biol. Psychiatry* **127**, 110807 (2023).
19. Lee, I. O. et al. The electroretinogram b-wave amplitude: a differential physiological measure for Attention Deficit Hyperactivity Disorder and Autism Spectrum Disorder. *J. Neurodev. Disord.* **14**, 30 (2022).
20. Dowling, J. E. *The Retina: An Approachable Part of the Brain*. (Harvard University Press, 1987).
21. Nguyen-Legros, J., Versaux-Botteri, C. & Vernier, P. Dopamine receptor localization in the mammalian retina. *Mol. Neurobiol.* **19**, 181–204 (1999).
22. Huemer, K.-H. et al. Effects of dopamine on retinal and choroidal blood flow parameters in humans. *Br. J. Ophthalmol.* **91**, 1194–1198 (2007).
23. Bhattacharya, R. et al. The neurotransmitter dopamine modulates vascular permeability in the endothelium. *J. Mol. Signal.* **3**, 14 (2008).
24. Cao, M., Martin, E. & Li, X. Machine learning in attention-deficit/hyperactivity disorder: new approaches toward understanding the neural mechanisms. *Transl. Psychiatry* **13**, 236 (2023).
25. Li, S. L. et al. The association between attention-deficit/hyperactivity disorder and retinal nerve fiber/ganglion cell layer thickness measured by optical coherence tomography: a systematic review and meta-analysis. *Int. Ophthalmol.* **41**, 3211–3221 (2021).
26. Kim, J. H. et al. Development of deep ensembles to screen for autism and symptom severity using retinal photographs. *JAMA Netw. Open* **6**, e2347692–e2347692 (2023).
27. Seo, J.-M., Lee, J.-S., Kim, S.-Y. & Kim, H.-W. Diagnostic Significance of Comprehensive Attention Test in Children and Adolescents with Attention-Deficit Hyperactivity Disorder. *J. Korean Acad. Child Adolesc. Psychiatry* **22**, 246–252 (2011).
28. Slobodin, O., Yahav, I. & Berger, I. A Machine-Based Prediction Model of ADHD Using CPT Data. *Front. Hum. Neurosci.* **14**, 560021 (2020).
29. Ghasemi, E., Ebrahimi, M. & Ebrahimi, E. Machine learning models effectively distinguish attention-deficit/hyperactivity disorder using event-related potentials. *Cogn. Neurodyn* **16**, 1335–1349 (2022).
30. Mueller, A. et al. Discriminating between ADHD adults and controls using independent ERP components and a support vector machine: a validation study. *Nonlinear Biomed. Phys.* **5**, 5 (2011).
31. Kim, S. et al. Machine-learning-based diagnosis of drug-naïve adult patients with attention-deficit hyperactivity disorder using mismatch negativity. *Transl. Psychiatry* **11**, 484 (2021).
32. Alkahtani, H., Aldhyani, T., Ahmed, Z. & Alqarni, A. Developing system-based artificial intelligence models for detecting the attention deficit hyperactivity disorder. *Mathematics* **11**, 4698 (2023).
33. Merzon, L. et al. Eye movement behavior in a real-world virtual reality task reveals ADHD in children. *Sci. Rep.* **12**, 20308 (2022).
34. Yoo, J. H. et al. Development of an innovative approach using portable eye tracking to assist ADHD screening: a machine learning study. *Front. Psychiatry* **15**, 1337595 (2024).
35. Zhao, K. et al. A dynamic graph convolutional neural network framework reveals new insights into connectome dysfunctions in ADHD. *NeuroImage* **246**, 118774 (2022).
36. Luo, Y., Alvarez, T. L., Halperin, J. M. & Li, X. Multimodal neuroimaging-based prediction of adult outcomes in childhood-onset ADHD using ensemble learning techniques. *NeuroImage Clin.* **26**, 102238 (2020).
37. Chen, I.-C., Chang, C.-L., Chang, M.-H. & Ko, L.-W. The utility of wearable electroencephalography combined with behavioral measures to establish a practical multi-domain model for facilitating the diagnosis of young children with attention-deficit/hyperactivity disorder. *J. Neurodev. Disord.* **16**, 62 (2024).
38. Akkaya, S. Assessment of the effect of attention-deficit hyperactivity disorder on choroidal thickness using spectral domain optical coherence tomography. *Beyoglu Eye J.* <https://doi.org/10.14744/bej.2021.09821> (2021).
39. Grönlund, M. A., Aring, E., Landgren, M. & Hellström, A. Visual function and ocular features in children and adolescents with attention deficit hyperactivity disorder, with and without treatment with stimulants. *Eye* **21**, 494–502 (2007).
40. Long, Y. et al. Distinct brain structural abnormalities in attention-deficit/hyperactivity disorder and substance use disorders: A comparative meta-analysis. *Transl. Psychiatry* **12**, 368 (2022).
41. Parlattini, V. et al. White matter alterations in Attention-Deficit/Hyperactivity Disorder (ADHD): a systematic review of 129 diffusion imaging studies with meta-analysis. *Mol. Psychiatry* **28**, 4098–4123 (2023).
42. London, A., Benhar, I. & Schwartz, M. The retina as a window to the brain—from eye research to CNS disorders. *Nat. Rev. Neurol.* **9**, 44–53 (2013).
43. Waxman, S. G. & Black, J. A. Retinal involvement in multiple sclerosis. *Neurology* **69**, 1562–1563 (2007).
44. Witkovsky, P. Dopamine and retinal function. *Doc. Ophthalmol.* **108**, 17–39 (2004).
45. Popova, E. Role of dopamine in distal retina. *J. Comp. Physiol. A* **200**, 333–358 (2014).
46. Kothmann, W. W., Massey, S. C. & O'Brien, J. Dopamine-Stimulated Dephosphorylation of Connexin 36 Mediates All Amacrine Cell Uncoupling. *J. Neurosci.* **29**, 14903–14911 (2009).
47. Mills, S. L. et al. Dopaminergic modulation of tracer coupling in a ganglion-amacrine cell network. *Vis. Neurosci.* **24**, 593–608 (2007).
48. Zhang, A., Jacoby, R. & Wu, S. M. Light- and dopamine-regulated receptive field plasticity in primate horizontal cells. *J. Comp. Neurol.* **519**, 2125–2134 (2011).
49. Klitten, L. L. et al. Localization and regulation of dopamine receptor D4 expression in the adult and developing rat retina. *Exp. Eye Res.* **87**, 471–477 (2008).
50. Huemer, K.-H. et al. Effects of dopamine on human retinal vessel diameter and its modulation during flicker stimulation. *Am. J. Physiol. -Heart Circ. Physiol.* **284**, H358–H363 (2003).
51. MacDonald, H. J., Kleppe, R., Szigetvari, P. D. & Haavik, J. The dopamine hypothesis for ADHD: An evaluation of evidence accumulated from human studies and animal models. *Front. Psychiatry* **15**, 1492126 (2024).
52. Misiak, B. et al. Peripheral blood inflammatory markers in patients with attention deficit/hyperactivity disorder (ADHD): A systematic review and meta-analysis. *Prog. Neuropsychopharmacol. Biol. Psychiatry* **118**, 110581 (2022).
53. Yue, T. et al. The role of inflammation in immune system of diabetic retinopathy: Molecular mechanisms, pathogenetic role and therapeutic implications. *Front. Immunol.* **13**, 1055087 (2022).
54. Zhang, W. et al. IL-6/STAT3 Pathway is Critically Involved in TNF-Alpha Induced Retinal Vascular Inflammation. *Invest. Ophthalmol. Vis. Sci.* **51**, 4962–4962 (2010).
55. Tezel, G., Li, L. Y., Patil, R. V. & Wax, M. B. TNF- α and TNF- α receptor-1 in the retina of normal and glaucomatous eyes. *Invest. Ophthalmol. Vis. Sci.* **42**, 1787–1794 (2001).
56. Constable, P. A., Lim, J. K. H. & Thompson, D. A. Retinal electrophysiology in central nervous system disorders. A review of human and mouse studies. *Front. Neurosci.* **17**, 1215097 (2023).
57. Volkow, N. D. et al. Methylphenidate decreased the amount of glucose needed by the brain to perform a cognitive task. *PLoS ONE* **3**, e2017 (2008).
58. Zhang, F. et al. Corticostriatal causality analysis in children and adolescents with attention-deficit/hyperactivity disorder. *Psychiatry Clin. Neurosci.* **78**, 291–299 (2024).
59. Lin, H.-Y. et al. Auditory and visual attention performance in children with ADHD: The Attentional Deficiency of ADHD Is Modality Specific. *J. Atten. Disord.* **21**, 856–864 (2017).
60. Moreno-García, I., Delgado-Pardo, G. & Roldán-Blasco, C. Attention and Response Control in ADHD: Evaluation through Integrated Visual

- and Auditory Continuous Performance Test. *Span. J. Psychol.* **18**, E1 (2015).
61. Mihali, A., Young, A. G., Adler, L. A., Halassa, M. M. & Ma, W. J. A Low-Level Perceptual Correlate of Behavioral and Clinical Deficits in ADHD. *Comput. Psychiatry* **2**, 141 (2018).
 62. Edelman, J. A. & Xu, K. Z. Inhibition of Voluntary Saccadic Eye Movement Commands by Abrupt Visual Onsets. *J. Neurophysiol.* **101**, 1222–1234 (2009).
 63. Munoz, D. P., Armstrong, I. T., Hampton, K. A. & Moore, K. D. Altered Control of Visual Fixation and Saccadic Eye Movements in Attention-Deficit Hyperactivity Disorder. *J. Neurophysiol.* **90**, 503–514 (2003).
 64. Lee, T. L., Yeung, M. K., Sze, S. L. & Chan, A. S. Eye-Tracking Training Improves Inhibitory Control in Children with Attention-Deficit/Hyperactivity Disorder. *Brain Sci.* **11**, 314 (2021).
 65. Psotta, R., Sarvestan, J., Valtr, L. & Ješina, O. Quiet eye training-based intervention can ameliorate inhibitory control but not visuospatial working memory in children with ADHD. *Brain Behav.* **13**, e3251 (2023).
 66. Provost, E. B. et al. Denser Retinal Microvascular Network Is Inversely Associated With Behavioral Outcomes and Sustained Attention in Children. *Front. Neurol.* **12**, 547033 (2021).
 67. Kaymak, D., Gündoğmuş, İ., Dalkiran, M., Küçükcilioğlu, M. & Uzun, Ö. Retinal Nerve Fiber Layer Thickness and Its Relationship With Executive Functions in Adult Attention Deficit Hyperactivity Disorder Patients. *Psychiatry Investig.* **18**, 1171–1179 (2021).
 68. Schrantee, A. et al. Age-Dependent Effects of Methylphenidate on the Human Dopaminergic System in Young vs Adult Patients With Attention-Deficit/Hyperactivity Disorder: A Randomized Clinical Trial. *JAMA Psychiatry* **73**, 955 (2016).
 69. Lee, J. S. et al. Regional cerebral blood flow in children with attention deficit hyperactivity disorder: Comparison before and after methylphenidate treatment. *Hum. Brain Mapp.* **24**, 157–164 (2005).
 70. Tarakcioglu, H. N. et al. Foveal avascular zone and vessel density in children with attention deficit hyperactivity disorder. *Int. Ophthalmol.* **40**, 1155–1162 (2020).
 71. Sanches, E. S. et al. Attention-Deficit/Hyperactivity Disorder Animal Model Presents Retinal Alterations and Methylphenidate Has a Differential Effect in ADHD versus Control Conditions. *Antioxidants* **12**, 937 (2023).
 72. Dastamooz, S. et al. A systematic review and meta-analysis on the ocular characteristics in children and adolescents with neurodevelopmental disorders. *Sci. Rep.* **13**, 19397 (2023).
 73. Faraone, S. V. & Larsson, H. Genetics of attention deficit hyperactivity disorder. *Mol. Psychiatry* **24**, 562–575 (2019).
 74. Ghirardi, L. et al. Genetic and environmental contribution to the overlap between ADHD and ASD trait dimensions in young adults: a twin study. *Psychol. Med.* **49**, 1713–1721 (2019).
 75. Bossuyt, P. M. et al. STARD 2015: An Updated List of Essential Items for Reporting Diagnostic Accuracy Studies. *Radiology* **277**, 826–832 (2015).
 76. Zhou, Y. et al. AutoMorph: Automated Retinal Vascular Morphology Quantification Via a Deep Learning Pipeline. *Transl. Vis. Sci. Technol.* **11**, 12 (2022).
 77. Zhou, Y. et al. A foundation model for generalizable disease detection from retinal images. *Nature* **622**, 156–163 (2023).
 78. Ahsan, M. M., Luna, S. A. & Siddique, Z. Machine-Learning-Based Disease Diagnosis: A Comprehensive Review. *Healthcare* **10**, 541 (2022).
 79. So, Y.-K., Noh, J.-S., Kim, Y.-S., Ko, S.-G. & Koh, Y.-J. The reliability and validity of Korean parent and teacher ADHD rating scale. *J. Korean Neuropsychiatr. Assoc.* 283–289 (2002).
 80. Lundberg, S. M. & Lee, S.-I. A Unified Approach to Interpreting Model Predictions. in *Advances in Neural Information Processing Systems* (eds. Guyon, I. et al.) vol. 30 (Curran Associates, Inc., 2017).

Acknowledgements

This study used datasets from the Open AI Dataset Project for 2022, funded by a grant from the Ministry of Science and ICT (1-029-079) and the National Information Society Agency (AI-Hub) of South Korea (Prof. Cheon). This research was supported by a grant from the MD-PhD/Medical Scientist Training Program through the Korea Health Industry Development Institute (KHIDI), funded by the Ministry of Health and Welfare, Republic of Korea, and by the Autism and Developmental Disorder Center, Severance Hospital, Yonsei University College of Medicine, Seoul, Republic of Korea. We would like to thank the participants and their families for their participation in this study.

Author contributions

H.C., J.H., and H.G.K. contributed equally to the study as co-first authors. H.C., H.G.K., S.Y., and K.C. conceptualized and designed the study. H.G.K., M.H.P., S.H., J.L., and K.C. contributed to data acquisition. J.H., D.K., and H.G.K. curated the data. J.H. and Y.R.P. developed and implemented the machine learning analysis. H.C., J.H., H.G.K., Y.R.P., and K.C. interpreted the data. H.C., J.H., and H.G.K. drafted the original manuscript, which was improved by M.H.P., S.H., J.L., S.Y., D.K., Y.R.P., and K.C. All authors critically reviewed and revised the manuscript and approved the final version for submission. YRP and KC have full access to all study data and take responsibility for data integrity and accuracy of analyses. All authors had full access to all the data in the study and reviewed the manuscript.

Competing interests

The authors declare no competing interests.

Additional information

Supplementary information The online version contains supplementary material available at <https://doi.org/10.1038/s41746-025-01547-9>.

Correspondence and requests for materials should be addressed to Yu Rang Park or Keun-Ah Cheon.

Reprints and permissions information is available at <http://www.nature.com/reprints>

Publisher's note Springer Nature remains neutral with regard to jurisdictional claims in published maps and institutional affiliations.

Open Access This article is licensed under a Creative Commons Attribution-NonCommercial-NoDerivatives 4.0 International License, which permits any non-commercial use, sharing, distribution and reproduction in any medium or format, as long as you give appropriate credit to the original author(s) and the source, provide a link to the Creative Commons licence, and indicate if you modified the licensed material. You do not have permission under this licence to share adapted material derived from this article or parts of it. The images or other third party material in this article are included in the article's Creative Commons licence, unless indicated otherwise in a credit line to the material. If material is not included in the article's Creative Commons licence and your intended use is not permitted by statutory regulation or exceeds the permitted use, you will need to obtain permission directly from the copyright holder. To view a copy of this licence, visit <http://creativecommons.org/licenses/by-nc-nd/4.0/>.

© The Author(s) 2025